

Supporting Information

Enhanced photocatalytic performances of SnS₂/TiO₂ composites via a charge separation following Z-scheme at the SnS₂/TiO₂{101} facets

Nkenku Carl ^a, Muhammad Fiaz ^b, Hyun-Seok Oh ^c, Yu Kwon Kim ^{d*}

^a Department of Energy Systems Research, Ajou University, Suwon, 16499, South

Korea, nkenkuc@gmail.com

^b Department of Chemistry, Ajou university, Suwon, 16499, South Korea, fiaz299@yahoo.com

^c Department of Energy Systems Research, Ajou University, Suwon, 16499, South

Korea, jejuohs@ajou.ac.kr

^d Department of Chemistry, Ajou university, Suwon, 16499, South Korea, yukwonkim@ajou.ac.kr

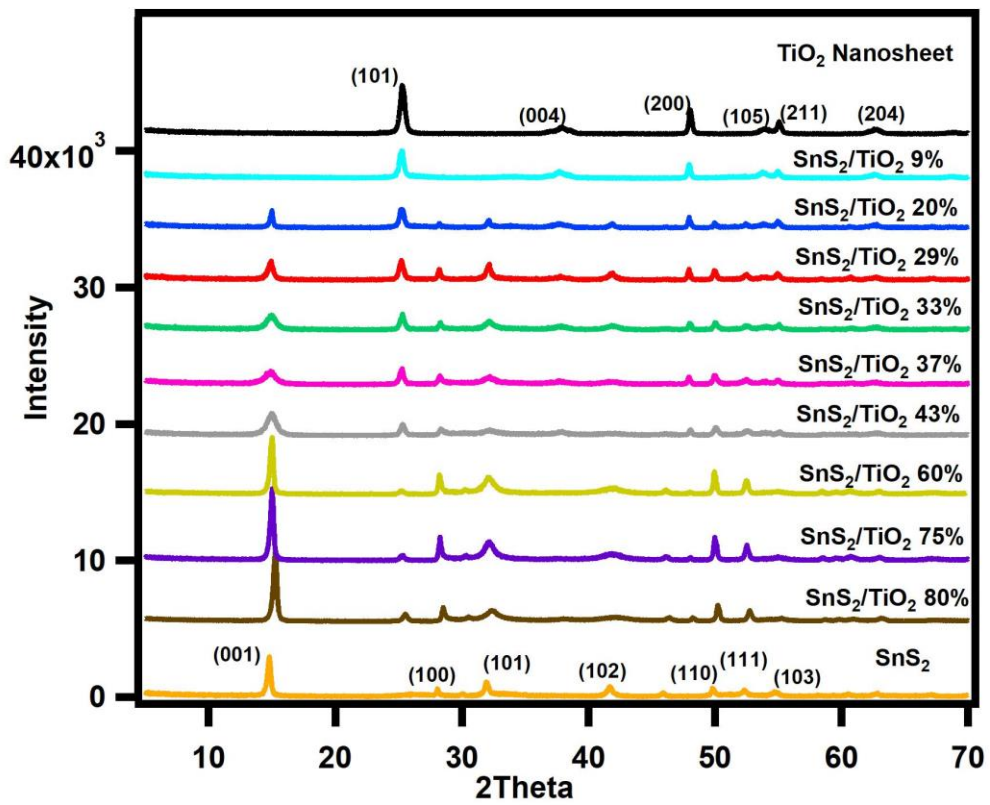


Figure S1. XRD patterns of as-prepared SnS_2 , TiO_2 Nanosheet, and $\text{SnS}_2/\text{TiO}_2$ heterojunction.

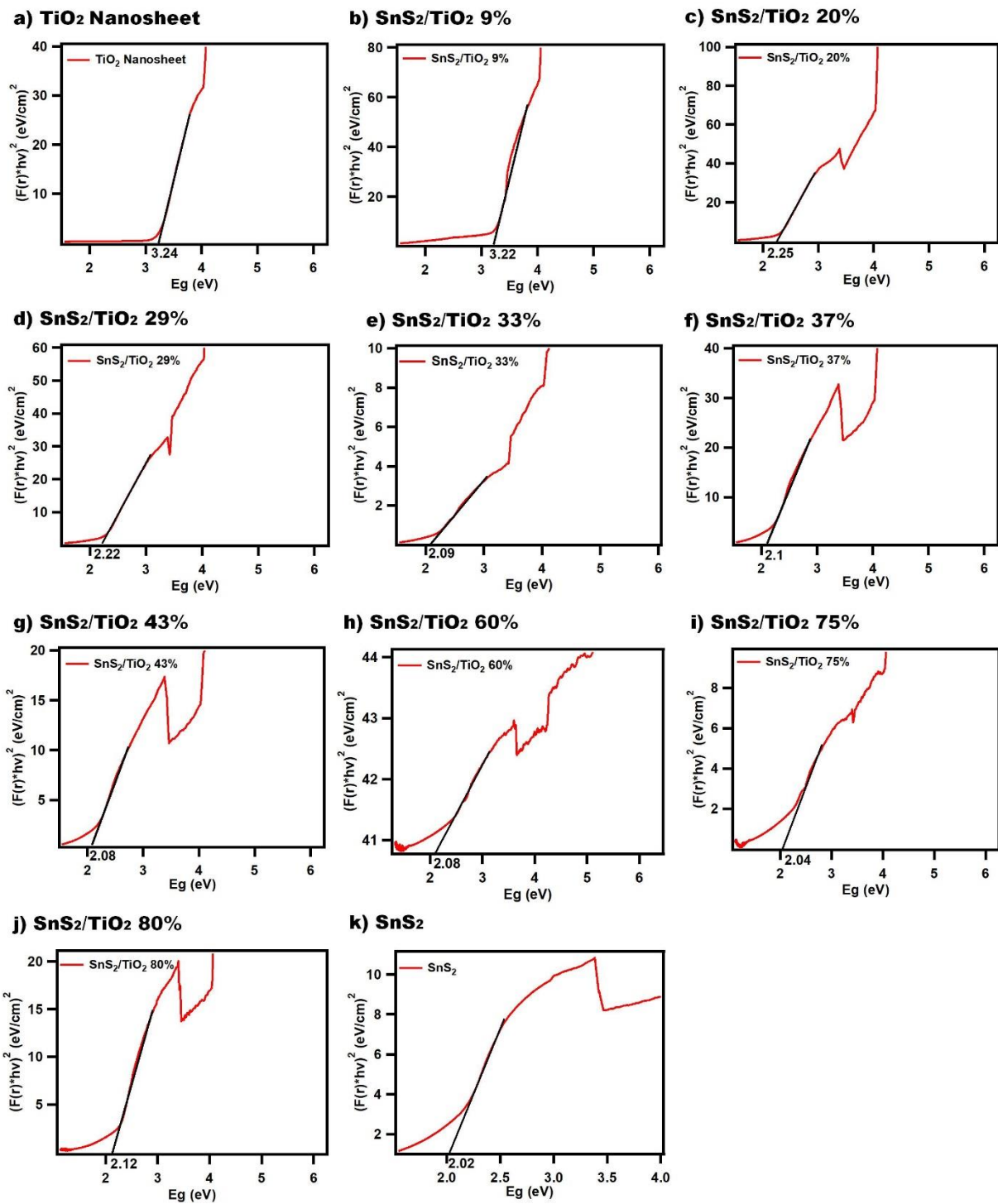


Figure S2. Bandgap energy plot Kubelka–Munk function for synthesis samples.

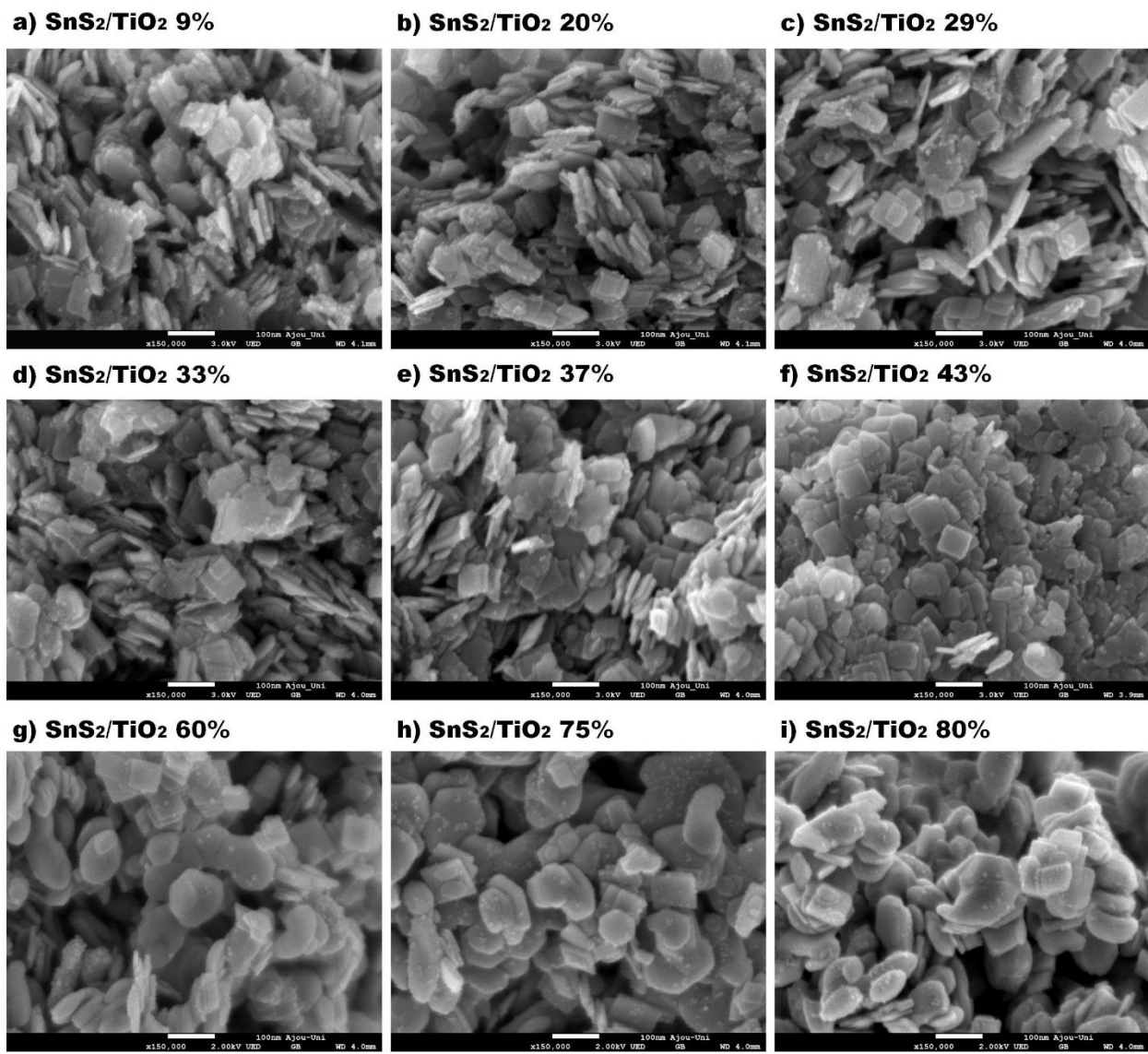


Figure S3. a-i shows SEM images of SnS₂/TiO₂ heterojunctions.

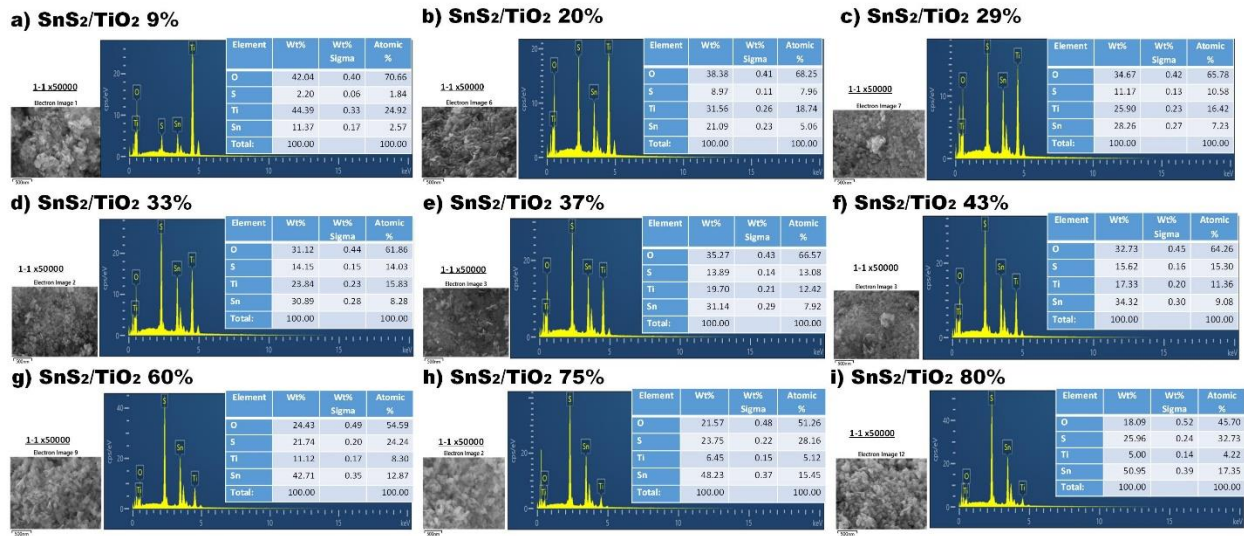
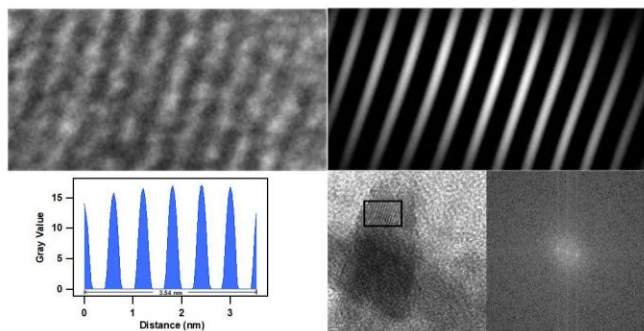


Figure S4. a-i shows EDS images of SnS₂/TiO₂ heterojunctions.

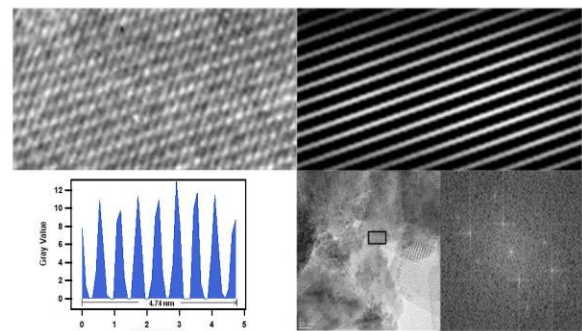
Table S1. %SnS₂ calculations from EDS data.

Sample Name	Ti (atomic %)	Sn (atomic %)	%SnS ₂
SnS ₂ /TiO ₂ 9%	24.92	2.57	9.35
SnS ₂ /TiO ₂ 20%	18.74	5.06	21.26
SnS ₂ /TiO ₂ 29%	16.42	7.23	30.57
SnS ₂ /TiO ₂ 33%	15.83	8.28	34.34
SnS ₂ /TiO ₂ 37%	12.42	7.92	38.94
SnS ₂ /TiO ₂ 43%	11.36	9.08	44.42
SnS ₂ /TiO ₂ 60%	8.30	12.87	60.79
SnS ₂ /TiO ₂ 75%	5.12	15.45	75.11
SnS ₂ /TiO ₂ 80%	4.10	16.68	80.27

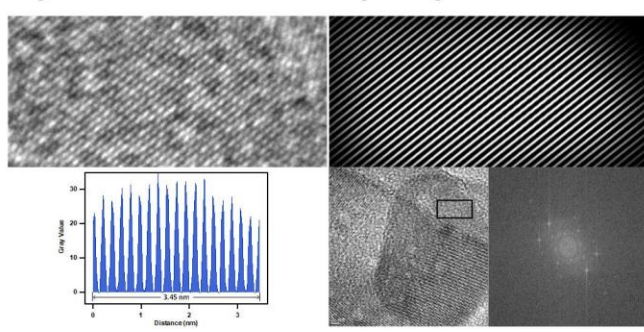
a) SnS₂ (001)



c) SnS₂/TiO₂ (SnS₂, 001)



b) TiO₂ Nanosheet (200)



d) SnS₂/TiO₂ (TiO₂, 101)

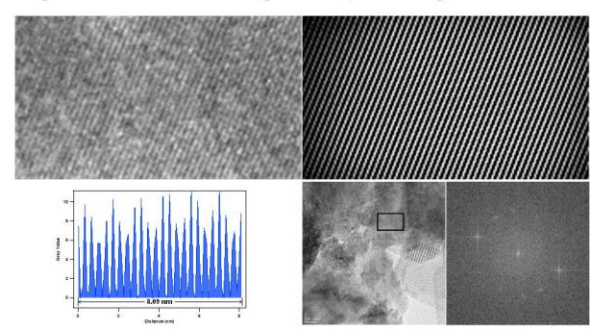
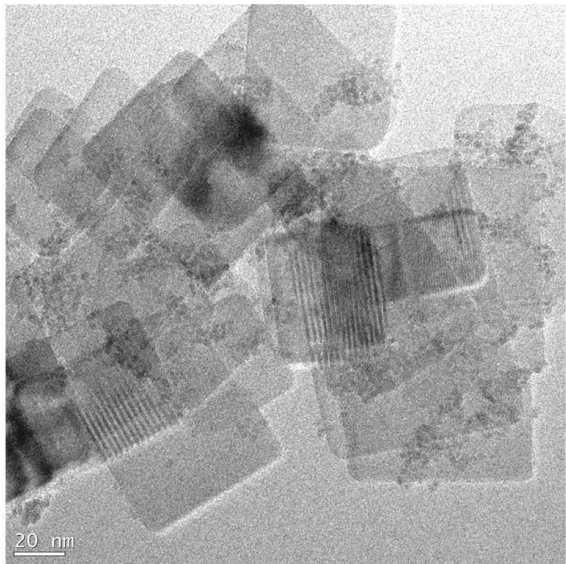


Figure S5. Profile of inverse fast fourier transformation (IFFT) for (a) Anatase TiO₂ nanosheet (200), (b) SnS₂ nanoparticles (001), (c) and (d) SnS₂/TiO₂ 43% (TiO₂ (101) and SnS₂ (001) respectively).

a) SnS₂/TiO₂ 33%



b) SnS₂/TiO₂ 43%

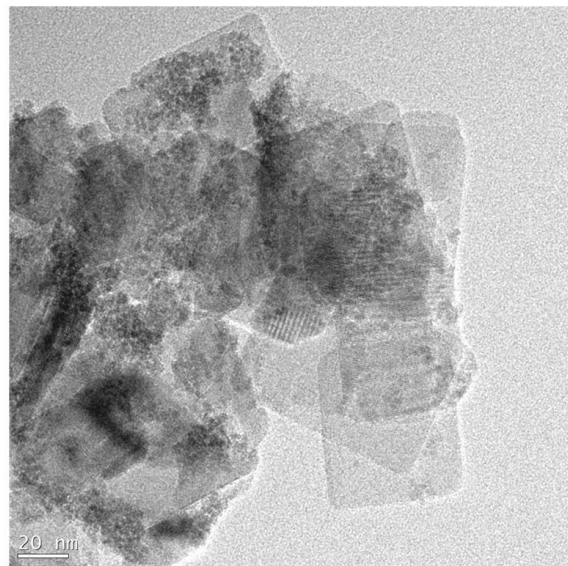


Figure S6. Increase content of SnS₂ nanoparticles for (a) SnS₂/TiO₂ 33% and (b) SnS₂/TiO₂ 43%

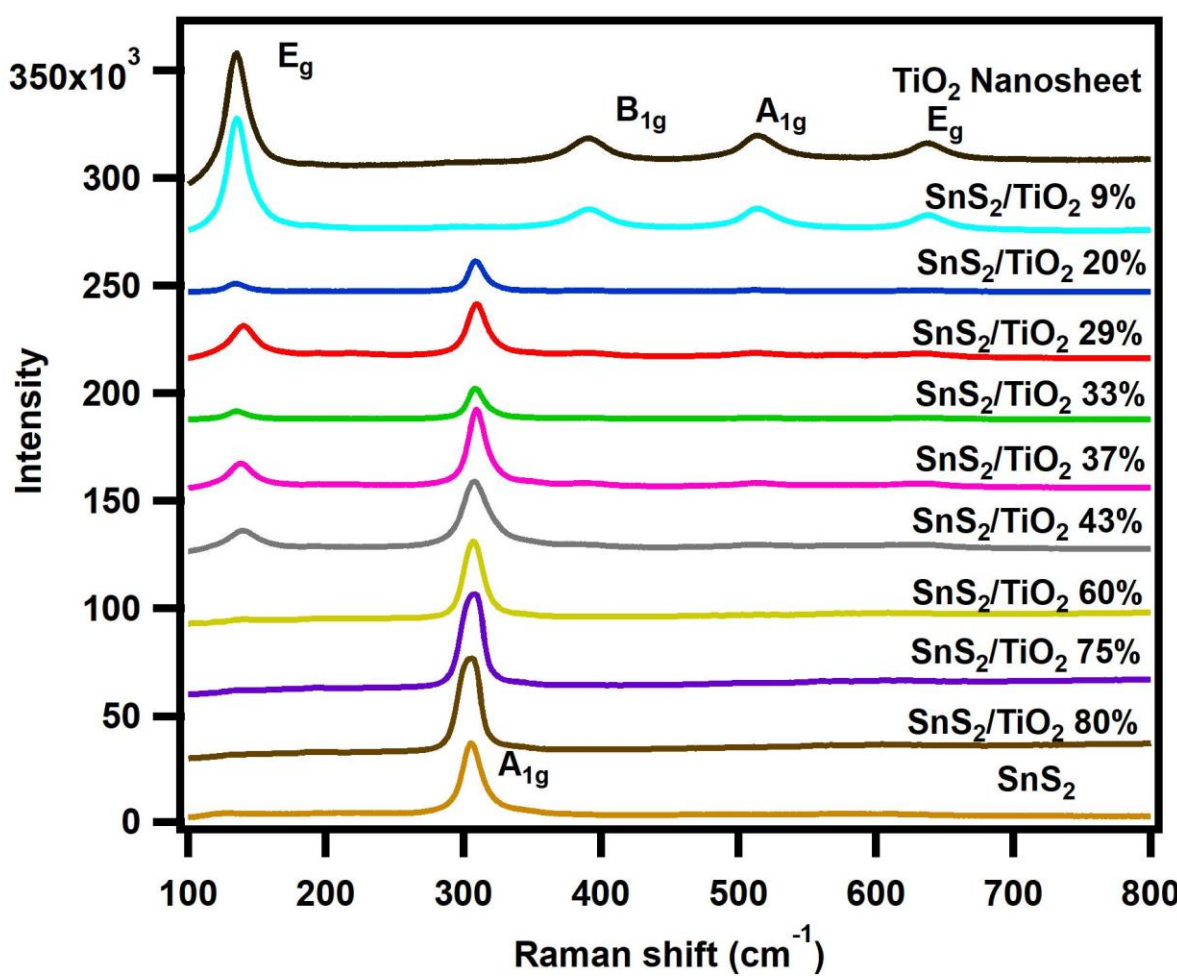


Figure S7. Raman spectra patterns of as-synthesis TiO_2 nanosheets, SnS_2 nanoparticles and $\text{SnS}_2/\text{TiO}_2$ heterojunctions.

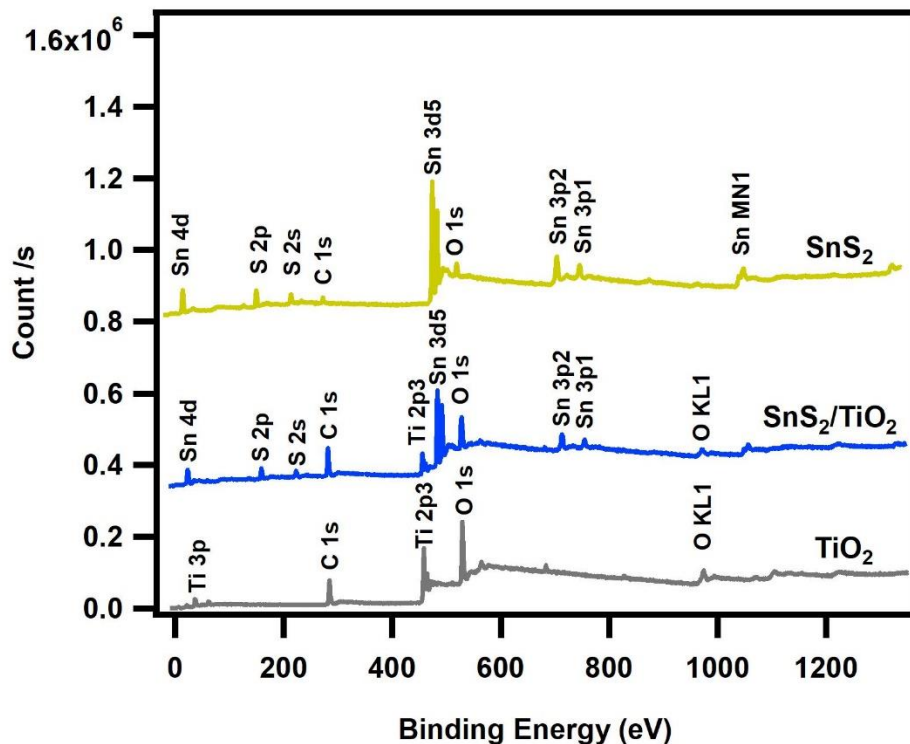


Figure S5. Survey Scan Spectra of as synthesis samples

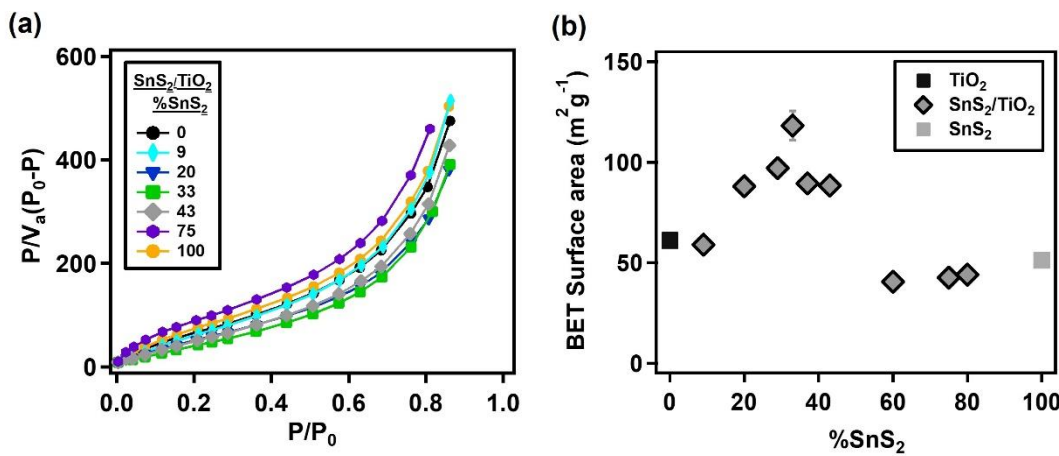


Figure S9. (a) BET N₂ adsorption isotherms and (b) the measured surface area of the SnS₂/TiO₂ composites, SnS₂ and TiO₂.

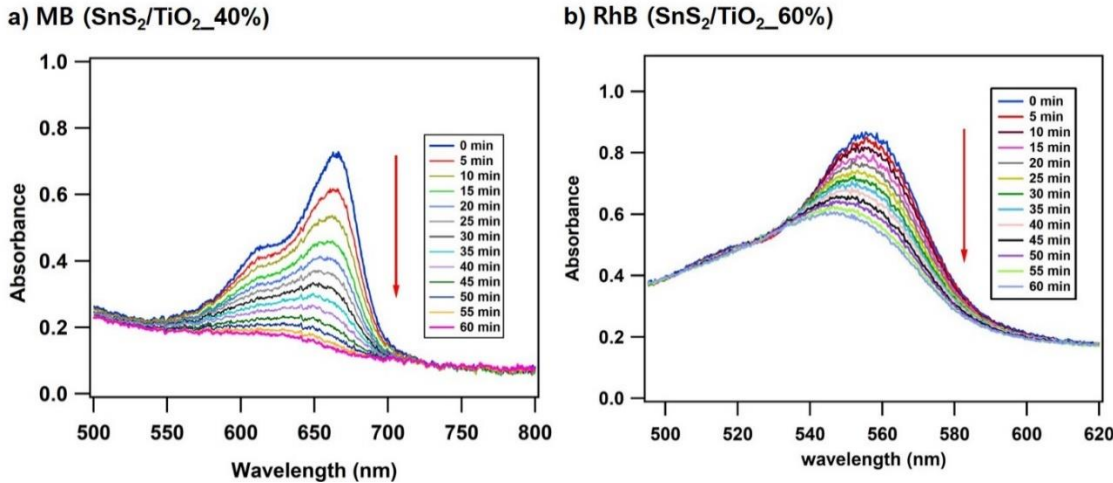


Figure S10. Typical absorbance for a) MB and b) RhB degradation under halogen lamp irradiation in the presence of SnS₂/TiO₂ shows a decrease in absorbance peak with time.

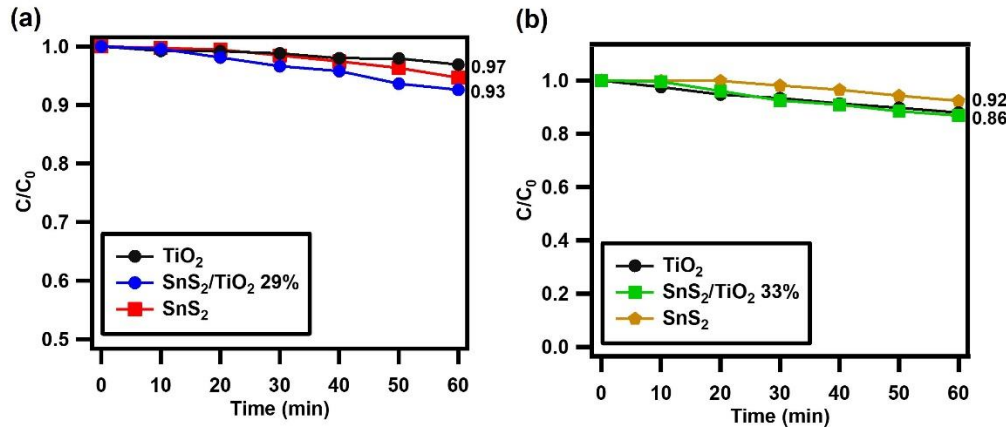


Figure S11. Photodegradation rates are shown as plots of C/C_0 vs time in the dark for (a) MB and (b) RhB.

The Conduction band and Valence band energy positions were calculated using equations 1 and 2 below [1,2].

$$E_{VB} = X - E_e + 0.5(E_g) \quad (S1)$$

$$E_{CB} = E_{VB} - E_g \quad (S2)$$

In equation 1, E_{VB} is the valence band edge potential, X is the absolute electronegativity, E_e energy of free electrons on the hydrogen scale (4.5eV vs NHE) and E_g is the bandgap of the semiconductor material,

in this case, SnS_2 and TiO_2 . The X value for SnS_2 is 4.66 eV[3], whereas that for TiO_2 is 5.9 eV [4]. Equation 2 uses EVB to calculate the conduction band edge potential. With these values, the band alignment can be represented as shown in Scheme 2.

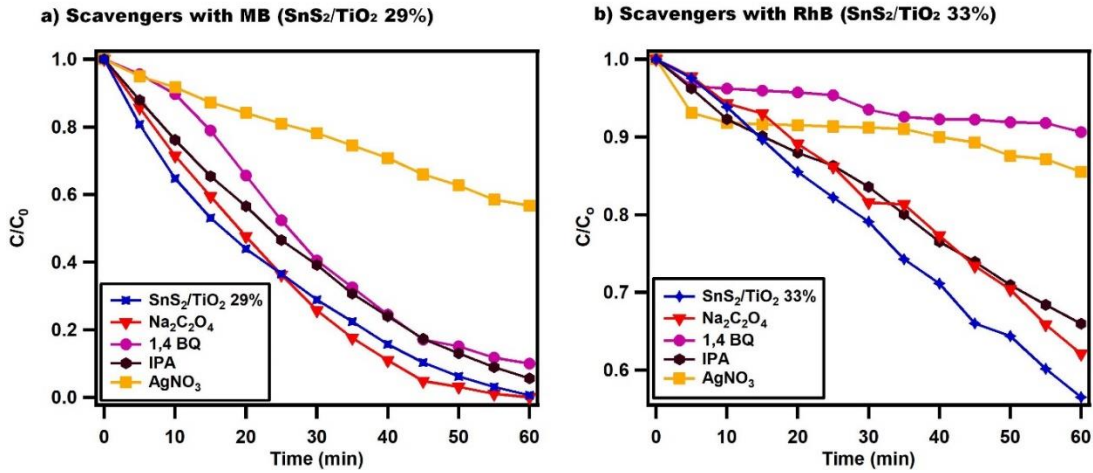


Figure S12. C/C_0 for Trapping experiment using MB ($\text{SnS}_2/\text{TiO}_2$ 29%) and RhB ($\text{SnS}_2/\text{TiO}_2$ 33%)

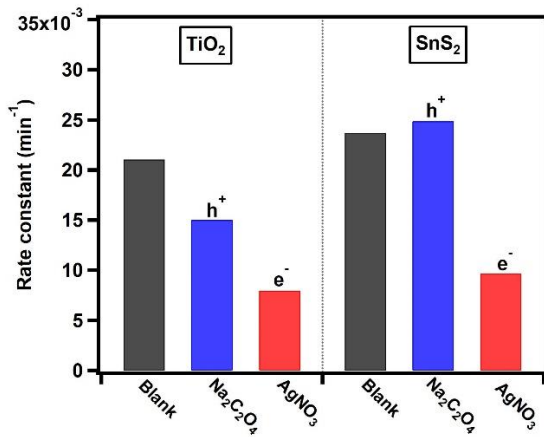


Figure S6. Rate constant for trapping experiment for using MB TiO_2 and SnS_2

References

1. Dai, X.; Xie, M.L.; Meng, S.G.; Fu, X.L.; Chen, S.F. Coupled systems for selective oxidation of aromatic alcohols to aldehydes and reduction of nitrobenzene into aniline using CdS/g-C₃N₄ photocatalyst under visible light irradiation. *Applied Catalysis B: Environmental* **2014**, *158*, 382-390, doi:<https://doi.org/10.1016/j.apcatb.2014.04.035>.
2. She, H.; Zhou, H.; Li, L.; Zhao, Z.; Jiang, M.; Huang, J.; Wang, L.; Wang, Q. Construction of a two-dimensional composite derived from TiO₂ and SnS₂ for enhanced photocatalytic reduction of CO₂ into CH₄. *ACS Sustainable Chemistry & Engineering* **2019**, *7*, 650-659, doi:<https://doi.org/10.1021/acssuschemeng.8b04250>.
3. Luo, J.; Zhou, X.; Zhang, J.; Du, Z. Fabrication and characterization of Ag₂CO₃/SnS₂ composites with enhanced visible-light photocatalytic activity for the degradation of organic pollutants. *RSC Advances* **2015**, *5*, 86705-86712, doi:<http://dx.doi.org/10.1039/C5RA18262J>.
4. Kuldeep, A.R.; Dhabbe, R.S.; Garadkar, K.M. Development of g-C₃N₄-TiO₂ visible active hybrid photocatalyst for the photodegradation of methyl orange. *Research on Chemical Intermediates* **2021**, *47*, 5155-5174, doi:<https://doi.org/10.1007/s11164-021-04561-0>.